FRONTIERS OF PHYSICS

RESEARCH ARTICLE
Volume 17 / Issue 5 / 53511 / 2022

Field-free switching through bulk spin–orbit torque in $L1_0$-FePt films deposited on vicinal substrates

Yongming Luo[1,†], Yanshan Zhuang[1], Zhongshu Feng[1], Haodong Fan[1], Birui Wu[1], Menghao Jin[1], Ziji Shao[1], Hai Li[1], Ru Bai[1], Yizheng Wu[2], Ningning Wang[1], Tiejun Zhou[1,‡]

1 Center for Integrated Spintronic Devices, Hangzhou Dianzi University, Hangzhou 310018, China
2 State Key Laboratory of Surface Physics and Department of Physics, Fudan University, Shanghai 200433, China
Corresponding authors. E-mail: †ymluo@hdu.edu.cn, ‡tjzhou@hdu.edu.cn
Received April 6, 2022; accepted July 5, 2022

ABSTRACT

$L1_0$-FePt distinguishes itself for its ultrahigh perpendicular magnetic anisotropy (PMA), enabling thermally stabile memory cells to scale down to 3 nm. The recently discovered "bulk" spin–orbit torques in $L1_0$-FePt provide an efficient and scalable way to manipulate the $L1_0$-FePt magnetization. However, the existence of an external field during the switching limits its practical application, and therefore field-free switching of $L1_0$-FePt is highly demanded. In this manuscript, by growing the $L1_0$-FePt film on vicinal MgO (001) substrates, we realize the field-free switching of $L1_0$-FePt. This method is different from previously established strategies as it does not need to add other functional layers or create asymmetry in the film structure. The dependence on the vicinal angle, film thickness, and growth temperature demonstrates a wide operation window for the field-free switching of $L1_0$-FePt. We confirm the physical origin of the field-free switching is due to the tilted anisotropy of $L1_0$-FePt induced by the vicinal surface. We also quantitatively characterize the spin-orbit torques in the $L1_0$-FePt films. Our results extend beyond the established strategies to realize field-free switching, and potentially could be applied to mass production.

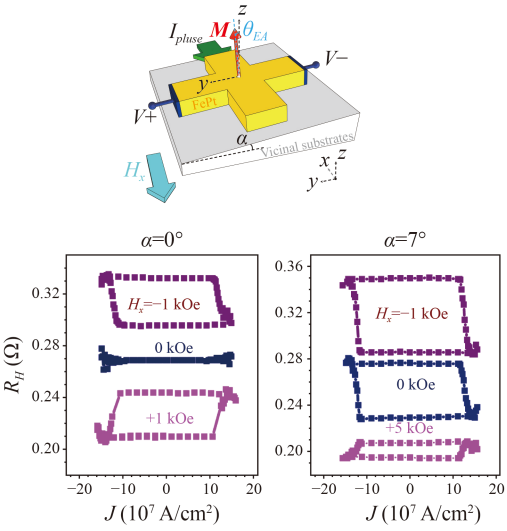

Keywords spin–orbit torque, vicinal substrates, field-free switching

1 Introduction

The FePt in $L1_0$ phase possesses one of the highest perpendicular magnetocrystalline anisotropy among transition metal compounds, which enables thermally stable devices to scale down to 3 nm and therefore distinguishes itself for vast applications, such as high-density magnetic recording, magnetic random access memory, and spin logic circuits [1]. However, the large anisotropy makes the switching of $L1_0$-FePt magnetization extremely challenging. Recent experiments have demonstrated that the $L1_0$-FePt could be switched by "bulk" like spin–orbit torques (SOT) in the single $L1_0$-FePt layer, which provides an efficient and scalable way to manipulate the $L1_0$-FePt magnetization electrically [2–5]. However, the deterministic switching of $L1_0$-FePt by SOT requires an external field being colinear with the current [6–8], which limit its practical applications [9]. Field-free switching of single $L1_0$-FePt film is highly demanded.

Previously studies have shown that field-free switching could be realized by tilting the perpendicular magnetization. To realize this, one way is to use the magnetic coupling effects by adding different functional layers, for

Higher Education Press

arXiv: 2203.06921
https://doi.org/10.1007/s11467-022-1197-7

example, by using interlayer coupling in a ferromagnet/nonmagnet/ferromagnet tri-layers [10], or by using exchange bias effects in ferromagnet/antiferromagnetic bilayers [11]. However, adding functional layers would often complex the device structure and result in instability [9]. Researchers also try to directly tune the anisotropy of the ferromagnetic layers without adding additional layers [12]. You *et al.* [13] first showed that using the shape-induced tilted anisotropy at the edge of a magnetic pillar could realize field-free switching. However, such artificially induced tilted-anisotropy needs a complex etching technique. Liu *et al.* [14] further found the tilted anisotropy in the $SrRuO_3$/$SrIrO_3$ bilayer system and demonstrated the field-free switching in such a system. Unfortunately, the $SrRuO_3$/$SrIrO_3$ system could only be operated at low temperatures due to its low Curie temperature.

Vicinal substrates denote those substrates with periodic atomic steps at the substrate surfaces. They are fabricated by inducing an inclination angle relative to the crystallographic plane during the cutting. Previously, it has been demonstrated that the periodic atomic steps on vicinal substrates could provide a unique way to tune the electronic or chemical properties of the films that are deposited on them, which has been a long-standing subject of intensive research [15, 16]. It is established that vicinal substrates could significantly influence the magnetic anisotropy of various ferromagnetic [17–19] and antiferromagnetic films [20, 21].

In this work, by growing the $L1_0$-FePt on vicinal MgO (001) substrates, we realize the field-free switching of the single $L1_0$-FePt film. We demonstrate that field-free switching is robust and able to withstand strong field disturbance due to an effective field of above 1 kOe induced by the vicinal substrates. Through AMR (Anisotropic Magneto-Resistance) measurements and micromagnetic simulation, we demonstrate that the field-free switching is due to the tilting of the easy axis of $L1_0$-FePt when grown on vicinal substrates. We further quantitatively characterize the effective spin–orbit field as a function of substrates' vicinal angle, film deposition temperature and film thickness, and the results indicate that the effective spin–orbit field has a similar "bulk" origin as that grown on flat substrates. Compared with the previously reported systems for tilted-anisotropy-induced field-free switching [13, 14], our approach is easier for mass production.

2 Result and discussion

2.1 Film characterization

$L1_0$-FePt is a face-centered tetragonal magnetic alloy, with Fe and Pt atoms alternatively stacked along the c axis, as schematically shown in Fig. 1(a). We grow our $L1_0$-FePt films by co-sputtering of Fe and Pt on flat or vicinal MgO (001) substrates at high temperatures (700 °C if not specified). The vicinal MgO (001) substrates are commercially obtained. AFM (Atomic Force Microscopy) measurements indicate that the surfaces of the vicinal substrates do not have any contaminations. Figure 1(b) schematically shows the period atomic steps of the vicinal substrate and the films grown on it. α denotes the vicinal angle of the substrates [shown in Fig. 1(b)]. The $L1_0$ phase and perpendicular anisotropy of the FePt films are confirmed by X-ray diffraction (XRD) patterns and normalized Hall resistance loops, respectively. Figure 1(c) shows the XRD spectrums of 6 nm FePt films grown on flat (α = 0 °) and vicinal (α = 7 °) MgO (001) substrates. For film grown on the flat substrate, strong FePt (001) and (002) peaks could be observed [black line in Fig. 1(c)], demonstrating the high-quality of the $L1_0$-FePt film. For the film grown on the vicinal substrate, although the intensity of the XRD spectrum (including the substrate peak) is drastically reduced by two orders compared with that grown on the flat substrate, the (001) FePt peak could still be observed [red line in Fig. 1(c)]. This demonstrated that the FePt film is still in the $L1_0$ phase, even though the chemical order is reduced compared with those grown on flat substrates [22]. The reduced XRD intensity may due to the atomic steps of the vicinal substrates. The magnetic properties of the FePt films are characterized by Anomalous Hall measurements. Figure 1(d) shows the anomalous Hall voltages of the FePt films grown on the flat and vicinal substrates. For both samples, the anomalous Hall signal exhibits square loops with large

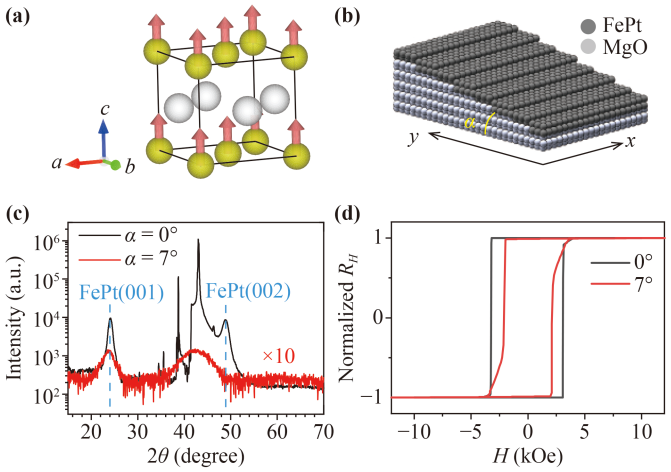

Fig. 1 **(a)** Atomic structure of the $L1_0$-FePt. The orange and gray spheres represent the Fe and Pt atoms, respectively, while the pink arrows represent the spin of the associated Fe atoms. **(b)** Schematic drawing of the FePt film grown on vicinal substrates. α denotes the vicinal angle of the substrates. **(c)** θ–2θ XRD spectra of the 6 nm $L1_0$-FePt films grown on flat (α = 0°) and vicinal (α = 7°) MgO (001) substrates. **(d)** Out-of-Plane normalized AHE loops of the 6 nm $L1_0$-FePt grown on flat and vicinal MgO (001) substrates.

coercivity (~ 3 kOe) when the field is swept along the out-of-plane direction, which is consistent with previously reported $L1_0$-FePt films [23]. However, a reduction of coercivity and a slight change of hysteresis-loop shape are seen, indicating a small change of magnetic properties for films deposited on vicinal substrates.

Due to the nature of an inclined surface for the vicinal substrates, it is plausible to assume that the easy axis of the $L1_0$-FePt film is slightly tilted away from the film normal, causing the change of magnetic properties when deposited onto vicinal substrates, which can be confirmed by anisotropic magnetoresistance (AMR) and micromagnetic simulations. Due to AMR effects, the longitudinal resistance along the current direction (R) can be written as

$$R(\theta) \propto R_{\perp} + (R_{//} - R_{\perp})\cos^2\phi(\theta), \quad (1)$$

where ϕ and θ are the angles of FePt magnetization and field relative to the current direction, respectively. $R_{\perp}$ and $R_{//}$ denote the resistance when the magnetization is perpendicular and parallel with the current, respectively. We pattern the FePt films (6 nm) into 35 μm × 5 μm bar structures for the AMR measurement. We measured the angular dependence of the R for samples grown on flat (sample #1, $\alpha = 0°$) and vicinal (sample #2, $\alpha = 7°$) substrates. Figure 2(a) schematically shows the set-up of the AMR measurements. An AC current (50 μA) is applied along the vicinal direction (y-axis). Fields with different amplitudes are rotated in the yz-plane from 0° to 360° (counterclockwise, CCW), and then rotated back from 360° to 0° (clockwise, CW). We plot the magnetoresistance, which is defined as $\Delta R = R - R_{\perp}$, as a function of θ. The results are shown in Fig. 2(c). We found both samples exhibit rotational hysteresis around the hard axis (perpendicular to the easy axis, around $\theta = 180°$), while their symmetries are different. For sample #1, the hysteresis is symmetric against $\theta = 180°$; while for sample #2, the hysteresis is asymmetric against $\theta = 180°$. The center of the hysteresis is shifted from $\theta = 180°$ (the offset is about 10°), and the peak values of ΔR are also asymmetric when the fields rotate CW and CCW. For both samples, the hysteresis becomes smaller and even disappear with increasing the applied field (up to 3 T). This is because when the field is high enough, the magnetization would rotate coherently with the field and the rotational asymmetry would disappear gradually.

Next, by using macrospin model and simulation, we demonstrate the asymmetric rotational hysteresis in sample #2 originates from the tilted anisotropy. In a system with uniaxial anisotropy, according to the macrospin model, when the field rotates from the easy axis to the hard axis (perpendicular to the easy axis), the magnetization would be lagged behind the field, which results in the rotational hysteresis when the field rotates across the hard axis CCW and CW. In addition,

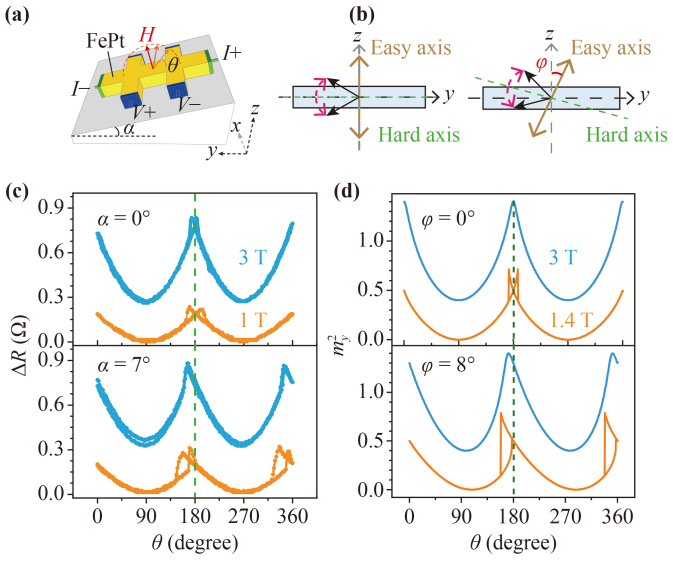

Fig. 2 AMR measurements for the $L1_0$-FePt films grown on flat and vicinal MgO substrates. **(a)** The schematic configuration of the AMR measurements. **(b)** The schematic drawing of the switching of magnetization when it rotates across the hard axis, for systems with different anisotropies. The left and right panels show switching processes with perpendicular (left) and tilted (right) anisotropies. **(c)** Angular dependence of ΔR for $L1_0$-FePt grown on different substrates. The field with different amplitudes is rotated from 0° to 360° (CCW), and then back from 360° to 0° (CW). The top and bottom panels represent the results for samples grown on flat ($\alpha = 0°$) and vicinal ($\alpha = 7°$) substrates respectively. **(d)** Simulation of the angular dependence of m_y^2 in systems with different directions of the easy axis. Fields with different amplitudes are rotated CCW, and then back CW. The top and bottom panels represent the results for samples with perpendicular ($\varphi = 0°$) and tilted anisotropy ($\varphi = 8°$), respectively. In **(c)** and **(d)**, the results at different fields are offset for clarity.

it should be noted that when the magnetization rotates across the hard axis CCW and CW, the switching of the magnetization should be symmetric. We consider two situations: (i) Perpendicular anisotropy, with the easy axis along the z-axis [situation #1, see the left panel of Fig. 2(b)]; (ii) Tilted anisotropy, with the easy axis tilted toward the y-axis [situation #2, see the right panel of Fig. 2(b)], and the tilted angle is defined as φ [shown in the right panel of Fig. 2(b)]. For situation #1, as the hard axis is colinear with the y-axis, the magnetization switching should be symmetric against the y-axis when the magnetization rotates across the y-axis CW and CCW, as schematically shown in the left panel of Fig. 2(b). The symmetric switching of the magnetization about the y-axis also leads to symmetric AMR hysteresis about $\theta = 180°$. This is because the AMR signal in Eq. (1) is related to the magnetization component along the current direction ($\sim m_y^2$) [10] for our AMR measurement geometry. While for situation #2, as the hard axis is not colinear with the y-axis, the magnetization switching

should be asymmetric about the y-axis [see the right panel of Fig. 2(b)], which would result in asymmetric AMR hysteresis. These features could be further confirmed by micromagnetic simulation. We simulated the rotation of the FePt magnetization when fields with different amplitudes are rotated in the yz-plane CW and CCW. The simulation details are shown in the supplementary information 4. We plot the angular dependence of the m_y^2 at different fields (1.4 T and 3 T) for two different systems with perpendicular ($\varphi = 0°$) and tilted ($\varphi = 8°$) anisotropy. The simulation results agree well with the macrospin analysis, as shown in Fig. 2(d). At low field (1.4 T), the rotational hysteresis of m_y^2 is symmetric (asymmetric) with respect to $\theta = 180°$ for situation #1 (situation #2). At high field (3 T), although the hysteresis disappears in both situations, the symmetry could still be observed. Compared with our AMR results [Fig. 2(c)], we could verify the hysteresis symmetry of sample #1 (sample #2) is well consistent with situation #1 (situation #2). The consistency between the experiment and theoretic analysis demonstrates that the easy axis of FePt is tilted away from the z-axis when grown on vicinal substrates, but fully perpendicular when it grown on the flat substrate. From the hysteresis shift, we can further estimate that the easy axis is tilted about 10° away from the film normal and along the vicinal direction for 6 nm FePt grown on the vicinal substrate ($\alpha = 7°$).

2.2 SOT switching characterization

Next, we demonstrate that the tilted anisotropy induced by vicinal substrates is critical to realize field-free SOT switching of the $L1_0$-FePt film. To electrically characterize the SOT switching of $L1_0$-FePt magnetization, we pattern the FePt films into Hall bar structures with 5 μm in width and 20 μm in length by using photolithography and argon ion milling. To drive the SOT switching of the $L1_0$-FePt magnetization, a DC pulse current I_{pluse} with a fixed duration of 30 μs along the x-direction is applied. After each pulse, the magnetization states of FePt film are read out by anomalous Hall resistance ($R_H = V_{ac}/I_{ac}$), by applying a small AC current ($I_{ac} = 50$ μA). Along the current direction, external fields with different amplitudes H_x are applied to help the switching, as schematically shown in Fig. 3(a). We compare the SOT switching behavior for films grown on flat and vicinal substrates. For films grown on flat substrates, we could observe typical SOT-induced magnetization switching, which is the same as what was reported previously [2, 3]. We observed the reversal of switching polarity when H_x changes from positive to negative, and no switching at zero fields (see in the supplementary information 1). While for FePt film grown on the vicinal substrate, as shown in Fig. 3(b), we also observed the SOT-induced switching of magnetization. Remarkably, we found that the SOT-induced

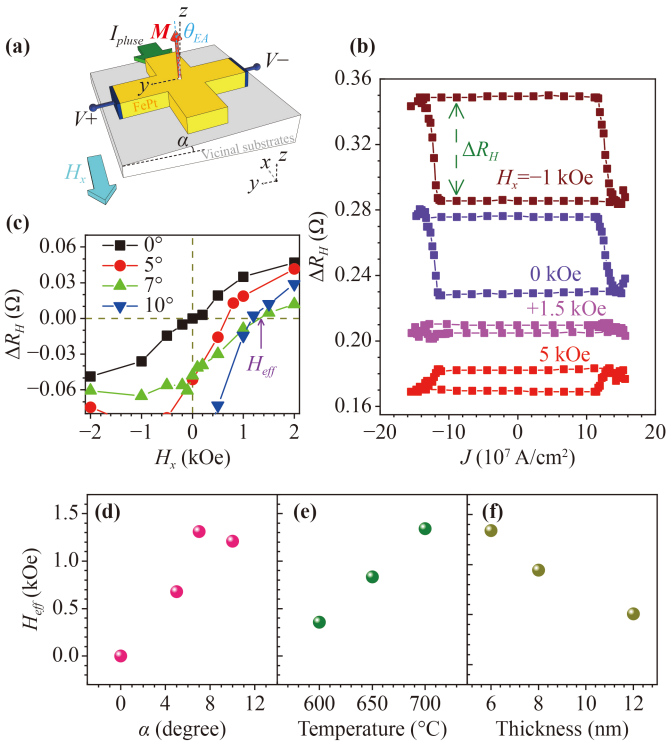

Fig. 3 Current-induced switching of the $L1_0$-FePt films grown on vicinal substrates. **(a)** Schematic drawing of the set-up for the current-induced magnetization switching of the $L1_0$-FePt films. **(b)** Current-induced magnetization switching of the 6 nm $L1_0$-FePt grown on the vicinal substrate ($\alpha = 7°$). The R_H at different H_x are offset for clarity. **(c)** Plot of ΔR_H as a function of H_x, for $L1_0$-FePt films grown on substrates with different vicinal angles. ΔR_H is marked by the green dash arrow in **(b)**. The dependence of H_{eff} with different parameters **(d)** Vicinal angles of the substrate, **(e)** Growth temperature and **(f)** The thickness of the $L1_0$-FePt film. If not specified, the vicinal angle for the vicinal substrates is 7°, the growth temperature of the $L1_0$-FePt film is 700 °C, and 6 nm in thickness.

switching can happen even at zero field, demonstrating the realization of field-free switching of the $L1_0$-FePt film. The switching polarity does not change until $H_x > 1.2$ kOe. These switching results indicate that the field-free switching of $L1_0$-FePt could withstand a strong field disturbance (~ 1.2 kOe), and the vicinal substrate could induce an in-plane effective field (H_{eff}) of 1.2 kOe. We found a partial switching behavior and the switching ratio is about 10 %, similar to the previously reported SOT switching of the single $L1_0$-FePt film [2, 3].

We also found that the field-free switching could not be realized when the pulse current was applied parallel to the vicinal direction (along the y-axis) (shown in the supplementary information 2). This feature demonstrates that the field-free SOT switching could only be observed when the current is perpendicular to the tilting direction of the easy axis [Fig. 3(a)]. Such switching property could be re-produced by micromagnetic simulation (shown in the supplementary information 4). The

consistency of experiment and simulation clearly demonstrated that the physical origin of field-free switching of the $L1_0$-FePt film is due to the tilted anisotropy. Such switching geometry is also in consistent with the previously reported field-free switching of the $SrRuO_3/SrIrO_3$ system [14].

In addition to substrates with vicinal angle $\alpha = 7°$, the field-free switching can also be achieved when FePt films are grown on substrates with other vicinal angles ($\alpha = 5°, 10°$). Figure 3(c) plots the change of SOT Hall resistance ΔR_H [marked in Fig. 3(b)] as a function of H_x for films grown on substrates with different vicinal angles ($\alpha = 0°, 5°, 7°, 10°$). The "±" signs of ΔR_H in Fig 3(c) denote CCW ("+") and CW ("–") switching polarity, while $\Delta R_H = 0$ denotes no switching could happen. For the film grown on the flat substrates ($\alpha = 0°$), we found that ΔR_H is an odd function of H_x with $\Delta R_H = 0$ at zero fields, implying that field-free switching does not happen. Furthermore, a H_x of less than 300 Oe is difficult to induce any observable change of ΔR_H. For films grown on vicinal substrates, we have $\Delta R_H \neq 0$ at zero fields, indicating the realization of field-free switching. The typical point where $\Delta R_H = 0$ ($H_x|_{\Delta R_H=0}$) reflects the effective field, H_{eff}, created by the vicinal substrate [marked in Fig. 3(c)]. For films grown on different vicinal substrates, we plot H_{eff} as a function of α, as shown in Fig. 3(d). We found H_{eff} first increases with α (from 0° to 7°) and then saturates at 7°, as H_{eff} at 7° and 10° samples are very close. It should be noted that the H_{eff} can be as high as 1.3 kOe, being much higher than that obtained from the established schemes for field free switching, such as adding an antiferromagnetic layer, or using a wedge-shaped film structure, where H_{eff} is typically about $50 - 100$ Oe [10, 11, 24, 25]. Besides, we also studied the switching behavior for FePt layer with different film thicknesses. As shown in Fig. 3(f), we found H_{eff} decreases almost linearly with the increasement of the film thickness, from ~ 1.3 kOe to 0.5 kOe when the FePt thickness increases from 6 nm to 12 nm, indicating the interface origin of H_{eff}. The dependence of H_{eff} on the vicinal angle (α) and film thickness implies that H_{eff} could be due to the interface strain from the vicinal substrates. In addition, we further explored the tunability of H_{eff} by controlling the chemical order of the FePt film [22]. As the XRD intensity of FePt film grown on vicinal substrates is very low, we could not directly calculate the chemical order of the film. We alternatively study the dependence of H_{eff} on the growth temperature, as it is established that the chemical order of FePt increases with the growth temperature [22]. As shown in Fig. 3(e), we found H_{eff} increase with growth temperature, indicating that the effective field is proportional to the chemical order. This could be attributed to higher lattice strain in films with high crystal order.

2.3 Second harmonic measurement

Next, we quantitatively characterize the current induced SOT field in $L1_0$-FePt films by harmonic Hall voltage analysis [26, 27]. We apply a small AC excitation current (with a density of J_e) and measure the first (V_ω) and second ($V_{2\omega}$) harmonic signals. Figure 4(a) shows the schematic drawing of the experiment set-up and the SOT effective fields ΔH_L and ΔH_T. Figures 3(b)–(d) plot the field dependence of V_ω and $V_{2\omega}$ signals for the 6 nm $L1_0$-FePt grown on the vicinal substrate ($\alpha = 7°$). We obtain the longitudinal (L) and transverse (T) spin-orbit fields by: $\Delta H_{L(T)} = -2\frac{B_{L(T)} \pm 2\xi B_{T(L)}}{1-4\xi^2}$, where $B_{L(T)}$ is defined as $\left(\frac{\partial V_{2\omega}}{\partial H} / \frac{\partial^2 V_\omega}{\partial H^2}\right)_{H_{L(T)}}$, and ξ is the ratio of the planar Hall voltage to the anomalous Hall voltage.

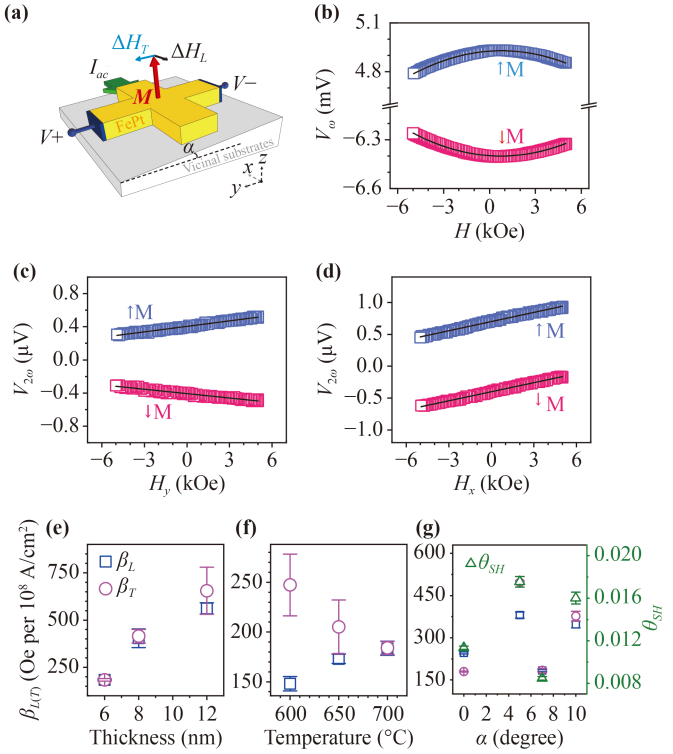

Fig. 4 Harmonic Hall voltage analysis of the $L1_0$-FePt films. **(a)** Schematic of the set-up for the Harmonic Hall voltage measurements, and illustration of the spin–orbit effective fields ΔH_L and ΔH_T. (b)–(d) are measurement results for the 6 nm $L1_0$-FePt film grown on the vicinal substrate. **(b)** First harmonic Hall voltage as a function of the longitudinal field H_x. Blue and pink squares are experimental data for the up and down magnetization directions, respectively. The solid lines are parabolic fits to the data. Second harmonic Hall voltages as a function of the transverse (H_y) **(c)** and longitudinal (H_x) fields **(d)**. The solid lines are linear fits to the data. For the data in (b)–(d), the AC current was 3 mA in amplitude. Dependence of spin-torque efficiencies ($\beta_{L(T)}$) with **(e)** Film Thickness, **(f)** Growth temperature and **(g)** Vicinal angles of the substrates (left). We also show the dependence of θ_{SH} with vicinal angles of the substrates in **(g)** (right). If not specified, the vicinal angle for the vicinal substrates is 7°, the growth temperature of the $L1_0$-FePt film is 700 °C, and 6 nm in thickness.

The $\pm$ sign corresponds to magnetization pointing along the $\pm z$-axis (i.e., $\pm M$), respectively [26, 27]. Previous studies have demonstrated that in the $L1_0$-FePt system, the thermoelectrical effects have a negligible influence on the value of $\frac{\partial V_{2\omega}}{\partial H}$ [3]. We, therefore, do not consider the influence of thermal effects. Our results show that $\Delta H_{L(T)}$ increases linearly with increasing current density J_e, and the symmetry of $\Delta H_L(\Delta H_T)$ is odd (even) with magnetization (See in the supplementary information 5), which are consistent with the previously reported current-induced effective fields in $L1_0$-FePt [2, 3]. We noted that for the ΔH_T measurement geometry, when the magnetization is upward and downward, the extracted value of $|\frac{\partial V_{2\omega}}{\partial H}|$ exist small discrepancy [Fig. 4(c)], this could be attributed to the Spin Seebeck effects (SSE) or Anomalous Nernst effect (ANE) [28]. To compare the SOT with previous studies, we further calculate the SOT efficiency $\beta_{L(T)}$, which is defined as $\frac{\Delta H_{L(T)}}{J_e}$. We characterize $\beta_{L(T)}$ for different FePt thicknesses, as shown in Fig. 4(e). We found that both β_L and β_T monotonically increase with the film thickness, demonstrating the "bulk" nature of the SOT. This result is self-consistent with a decreased critical SOT switching current density, for the $L1_0$-FePt with larger thickness (see in the supplementary information 3). The amplitudes of $\beta_{L(T)}$ are also comparable to the previous results [2, 3]. These features demonstrate that the origin of SOT for our FePt films is the same as that grown on flat substrates. We also characterize the dependence of $\beta_{L(T)}$ on the growth temperature, which reflect the relation between $\beta_{L(T)}$ and the chemical order of the film. As shown in Fig. 4(f), we found that β_L and β_T have opposite temperature dependence, with β_L increasing with growth temperature, while β_T decreasing with growth temperature. β_T is larger than β_L at low growth temperatures, while β_T and β_L have comparable values at high growth temperature. Although previous results have shown that β_L can be either larger [3] or smaller than β_T [2], both the β_T and β_L would increase with growth temperature. Our results are different from the previous findings. The underlying physics is not well understood and further experimental and theoretical investigations are needed to better understand the observed results.

So far, the micro-origin of the bulk SOT in FePt remains unsettled. Although experiments from different groups have demonstrated that the composition gradient in the film structures might play a critical role in generating the SOT in FePt [2–4], how the composition gradient breaks the inversion symmetry and results in a non-vanishing torque remains open. It is argued that the composition gradient could induce asymmetry of various SOT related parameters, such as spin–orbit coupling strength, magnetic exchange, the local density of states and magnetic moment density, all of which are expected to result in a local imbalance of spin current in the structure and to produce a non-vanishing torque. However, it is unclear which of them plays a dominating role. A thorough understanding of such bulk SOT is still lacking. On the other hand, recent studies have suggested the strain could play an important role in generating the bulk SOT. Zhu *et al.* [4] suggested that the non-uniform strain gradient induced by the composition gradient is most likely the origin of the bulk SOT in FePt films, as they found that the temperature dependence of the SOT efficiency is in accordance with the strain, rather than other parameters. Therefore, the strain-related effects, including strain itself and its gradient, might play an important role in the bulk SOT found in single layer $L1_0$-FePt films.

The vicinal substrates could provide a unique way to control the lattice strain for the films deposited on it. For the films deposited on the vicinal substrates, the periodic atomic steps could provide an additional strain. We characterize the $\beta_{L(T)}$ for films grown on vicinal substrates with different vicinal angles ($\alpha = 0°, 5°, 7°, 10°$). The results are shown in Fig. 4(g). Our results show that compared with the sample that is grown on a flat substrate ($\alpha = 0°$), β_L and β_T are obviously enhanced for samples with $\alpha = 5°$ and $10°$ while the sample with $\alpha = 7°$ is not enhanced too much. We further calculate the spin Hall angle (θ_{SH}) according to the formula $\theta_{SH} = \left(\frac{2e}{\hbar}\right)\mu_0 M_S t_{FM} \beta_{DL}$, where e, $\hbar$ and μ_0 are the elementary charge, reduced Planck constant and permeability of vacuum, respectively. M_S and t_{FM} are the saturation magnetization and thickness of the FePt film. The M_S of our FePt samples are determined by Vibrating Sample Magnetometer ($M_S = 1 \times 10^6$ A/m for our FePt films, shown in the supplementary information 6). The calculated θ_{SH} is below 0.02, while the typical value of Pt is 0.1 [29]. The θ_{SH} of our FePt films are smaller than Pt, which is in accordance with previously reported results for the bulk SOT in $L1_0$-FePt films [4]. Our results showed that the $\beta_{L(T)}$ does not have simple monotonous dependence on α. Although the exact mechanism for such behavior is not well understood, the competition among different strain effects that existed in the vicinal substrates might play a role. The strain from vicinal substrates would influence the SOT in FePt from two aspects, i.e., the strain induced by the vicinal substrate and such strain-induced change of strain-gradient along film normal direction. First, the strain induced by the vicinal substrates would influence the spin–orbit coupling, crystal symmetry, and orbital polarization, leading to the change of SOT in the $L1_0$-FePt films [30]. Second, similar with what was suggested by Zhu *et al.* [4], the change of strain gradient along out-of-plane direction would alter the SOT in the film as well. The two effects might work together or compete with each other, resulting in a non-monotonous dependence of $\beta_{L(T)}$ on α as observed in Fig. 4(g).

In addition, apart from the spin current generated by the spin Hall effects, recent work has shown that orbit

transfer torque (OTT), which uses the orbital magnetic moments, could also be effective for field-free switching of perpendicular magnetization [31, 32]. It has been reported that the lattice strain could influence orbital polarization/moment of a magnetic system [30], and therefore the lattice strain induced by the vicinal substrate might also induce a non-vanishing orbital current, that generates a similar orbit transfer torque, helping the field-free switching of FePt magnetization. However detailed investigations are needed to understand the possible contribution from the OTT in $L1_0$-FePt films, which may form a future research topic.

3 Conclusion

In summary, our results present an artificial way to realize tilted perpendicular anisotropy in $L1_0$-FePt film, which can be used to realize the field-free switching of the $L1_0$-FePt film. The switching can withstand a strong field disturbance (above 1 kOe), which is much larger than most of other established schemes. The dependence on the vicinal angle, film thickness, and growth temperature demonstrated that the operation window for field-free switching of $L1_0$-FePt is wide. Compared with the previously reported strategies for the tilted-anisotropy induced field-free switching [13, 14], our method is easier to fabricate and suitable for mass production. Furthermore, such a method could be potentially applied to other magnetic and even antiferromagnetic systems, as it is established that the vicinal substrates could tune the magnetic anisotropy of various magnetic and antiferromagnetic materials [20, 31, 33].

Notes: We notice a similar letter covering the same topic during the review process [34].

Electronic supplementary material The supplementary material is available in the online version of this article at https://doi.org/10.1007/s11467-022-1197-7 and https://journal.hep.com.cn/fop/EN/pdf/10.1007/s11467-022-1197-7 and is accessible for authorized users.

Acknowledgements We thank Drs. Xuefeng Zhang, Jian Zhang, Lianze Ji, Shuai Huang for their help of lithography, XRD characterization and helpful discussion. This work was supported by the "Pioneer" and "Leading Goose " RD Program of Zhejiang Province (Grant No. 2022C01053), the National Natural Science Foundation of China (Grant No. 12274108, 11874135 and 12104119), the Key Research and Development Program of Zhejiang Province (Grant No. 2021C01039), and the Natural Science Foundation of Zhejiang Province, China (Grant Nos. LQ20F040005 and LQ21A050001).

References

1. S. Sun, C. B. Murray, D. Weller, L. Folks, and A. Moser, Monodisperse FePt nanoparticles and ferromagnetic FePt nanocrystal superlattices, *Science* 287(5460), 1989 (2000)
2. M. Tang, K. Shen, S. Xu, H. Yang, S. Hu, W. Lü, C. Li, M. Li, Z. Yuan, S. J. Pennycook, K. Xia, A. Manchon, S. Zhou, and X. Qiu, Bulk spin torque-driven perpendicular magnetization switching in $L1_0$ FePt single layer, *Adv. Mater.* 32(31), 2002607 (2020)
3. L. Liu, J. Yu, R. Gonzalez-Hernandez, C. Li, J. Deng, W. Lin, C. Zhou, T. Zhou, J. Zhou, H. Wang, R. Guo, H. Y. Yoong, G. M. Chow, X. Han, B. Dupé, J. Železný, J. Sinova, and J. Chen, Electrical switching of perpendicular magnetization in a single ferromagnetic layer, *Phys. Rev. B* 101(22), 220402 (2020)
4. L. Zhu, D. C. Ralph, and R. A. Buhrman, Unveiling the mechanism of bulk spin−orbit torques within chemically disordered Fe_xPt_{1-x} single layers, *Adv. Funct. Mater.* 31(36), 2103898 (2021)
5. S. Q. Zheng, K. K. Meng, Q. B. Liu, J. K. Chen, J. Miao, X. G. Xu, and Y. Jiang, Disorder dependent spin-orbit torques in $L1_0$ FePt single layer, *Appl. Phys. Lett.* 117(24), 242403 (2020)
6. I. Mihai Miron, G. Gaudin, S. Auffret, B. Rodmacq, A. Schuhl, S. Pizzini, J. Vogel, and P. Gambardella, Current-driven spin torque induced by the Rashba effect in a ferromagnetic metal layer, *Nat. Mater.* 9(3), 230 (2010)
7. L. Liu, O. J. Lee, T. J. Gudmundsen, D. C. Ralph, and R. A. Buhrman, Current-induced switching of perpendicularly magnetized magnetic layers using spin torque from the spin Hall effect, *Phys. Rev. Lett.* 109(9), 096602 (2012)
8. L. Liu, C. F. Pai, Y. Li, H. W. Tseng, D. C. Ralph, and R. A. Buhrman, Spin-torque switching with the giant spin Hall effect of tantalum, *Science* 336(6081), 555 (2012)
9. Q. Shao, P. Li, L. Liu, H. Yang, S. Fukami, A. Razavi, H. Wu, K. Wang, F. Freimuth, Y. Mokrousov, M. D. Stiles, S. Emori, A. Hoffmann, J. Akerman, K. Roy, J. P. Wang, S. H. Yang, K. Garello, and W. Zhang, Roadmap of spin−orbit torques, *IEEE Trans. Magn.* 57(7), 1 (2021)
10. W. Kong, C. Wan, X. Wang, B. Tao, L. Huang, C. Fang, C. Guo, Y. Guang, M. Irfan, and X. Han, Spin-orbit torque switching in a T-type magnetic configuration with current orthogonal to easy axes, *Nat. Commun.* 10(1), 233 (2019)
11. S. Fukami, C. Zhang, S. DuttaGupta, A. Kurenkov, and H. Ohno, Magnetization switching by spin−orbit torque in an antiferromagnet−ferromagnet bilayer system, *Nat. Mater.* 15(5), 535 (2016)
12. K. Eason, S. G. Tan, M. B. A. Jalil, and J. Y. Khoo, Bistable perpendicular switching with in-plane spin polarization and without external fields, *Phys. Lett. A* 377(37), 2403 (2013)
13. L. You, O. Lee, D. Bhowmik, D. Labanowski, J. Hong, J. Bokor, and S. Salahuddin, Switching of perpendicularly polarized nanomagnets with spin−orbit torque without an external magnetic field by engineering a tilted anisotropy, *Proc. Natl. Acad. Sci. USA* 112(33), 10310 (2015)
14. L. Liu, Q. Qin, W. Lin, C. Li, Q. Xie, S. He, X. Shu, C. Zhou, Z. Lim, J. Yu, W. Lu, M. Li, X. Yan, S. J.

Pennycook, and J. Chen, Current-induced magnetization switching in all-oxide heterostructures, *Nat. Nanotechnol.* 14(10), 939 (2019)

15. F. Leroy, P. Mueller, J. J. Metois, and O. Pierre-Louis, Vicinal silicon surfaces: From step density wave to faceting, *Phys. Rev. B* 76(4), 045402 (2007)
16. C. Tegenkamp, Vicinal surfaces for functional nanostructures, *J. Phys.: Condens. Matter* 21(1), 013002 (2009)
17. S. Ma, A. Tan, J. X. Deng, J. Li, Z. D. Zhang, C. Hwang, and Z. Q. Qiu, Tailoring the magnetic anisotropy of Py/Ni bilayer films using well aligned atomic steps on Cu(001), *Sci. Rep.* 5(1), 1 (2015)
18. R. K. Kawakami, E. J. Escorcia-Aparicio, and Z. Q. Qiu, Symmetry-induced magnetic anisotropy in Fe films grown on stepped Ag(001), *Phys. Rev. Lett.* 77(12), 2570 (1996)
19. S. Dhesi, H. Dürr, and G. Van der Laan, Canted spin structures in Ni films on stepped Cu(001), *Phys. Rev. B* 59(13), 8408 (1999)
20. J. Choi, J. Wu, Y. Z. Wu, C. Won, A. Scholl, A. Doran, T. Owens, and Z. Q. Qiu, Effect of atomic steps on the interfacial interaction of FeMn/Co films grown on vicinal Cu(001), *Phys. Rev. B* 76(5), 054407 (2007)
21. J. Zhu, Q. Li, J. X. Li, Z. Ding, J. H. Liang, X. Xiao, Y. M. Luo, C. Y. Hua, H. J. Lin, T. W. Pi, Z. Hu, C. Won, and Y. Z. Wu, Antiferromagnetic spin reorientation transition in epitaxial NiO/CoO/MgO(001) systems, *Phys. Rev. B* 90(5), 054403 (2014)
22. P. He, L. Ma, Z. Shi, G. Guo, J. G. Zheng, Y. Xin, and S. Zhou, Chemical composition tuning of the anomalous Hall effect in isoelectronic $L1_0$ $FePd_{1-x}Pt_x$ alloy films, *Phys. Rev. Lett.* 109(6), 066402 (2012)
23. S. Okamoto, N. Kikuchi, O. Kitakami, T. Miyazaki, Y. Shimada, and K. Fukamichi, Chemical-order-dependent magnetic anisotropy and exchange stiffness constant of FePt (001) epitaxial films, *Phys. Rev. B* 66(2), 024413 (2002)
24. Z. Zhao, A. K. Smith, M. Jamali, and J. P. Wang, External-field-free spin Hall switching of perpendicular magnetic nanopillar with a dipole-coupled composite structure, *Adv. Electron. Mater.* 6(5), 1901368 (2020)
25. A. van den Brink, G. Vermijs, A. Solignac, J. Koo, J. T. Kohlhepp, H. J. M. Swagten, and B. Koopmans, Fieldfree magnetization reversal by spin-Hall effect and exchange bias, *Nat. Commun.* 7(1), 1 (2016)
26. M. Hayashi, J. Kim, M. Yamanouchi, and H. Ohno, Quantitative characterization of the spin-orbit torque using harmonic Hall voltage measurements, *Phys. Rev. B* 89(14), 144425 (2014)
27. K. Garello, I. M. Miron, C. O. Avci, F. Freimuth, Y. Mokrousov, S. Blügel, S. Auffret, O. Boulle, G. Gaudin, and P. Gambardella, Symmetry and magnitude of spin-orbit torques in ferromagnetic heterostructures, *Nat. Nanotechnol.* 8(8), 587 (2013)
28. C. O. Avci, A. Quindeau, C. F. Pai, M. Mann, L. Caretta, A. S. Tang, M. C. Onbasli, C. A. Ross, and G. S. Beach, Current-induced switching in a magnetic insulator, *Nat. Mater.* 16(3), 309 (2017)
29. L. Zhu, D. C. Ralph, and R. A. Buhrman, Maximizing spinorbit torque generated by the spin Hall effect of Pt, *Appl. Phys. Rev.* 8(3), 031308 (2021)
30. M. Filianina, J. P. Hanke, K. Lee, D. S. Han, S. Jaiswal, A. Rajan, G. Jakob, Y. Mokrousov, and M. Kläui, Electric-field control of spin-orbit torques in perpendicularly magnetized W/CoFeB/MgO films, *Phys. Rev. Lett.* 124(21), 217701 (2020)
31. X. G. Ye, P. F. Zhu, W. Z. Xu, N. Shang, K. Liu, and Z. M. Liao, Orbit-transfer torque driven field-free switching of perpendicular magnetization, *Chin. Phys. Lett.* 39(3), 037303 (2022)
32. D. Lee, D. Go, H. J. Park, W. Jeong, H. W. Ko, D. Yun, D. Jo, S. Lee, G. Go, J. H. Oh, K. J. Kim, B. G. Park, B. C. Min, H. C. Koo, H. W. Lee, O. J. Lee, and K. J. Lee, Orbital torque in magnetic bilayers, *Nat. Commun.* 12(1), 6710 (2021)
33. P. Perna, C. Rodrigo, E. Jiménez, N. Mikuszeit, F. J. Teran, L. Méchin, J. Camarero, and R. Miranda, Magnetization reversal in half metallic $La_{0.7}Sr_{0.3}MnO_3$ films grown onto vicinal surfaces, *J. Appl. Phys.* 109, 07B107 (2011)
34. Y. Tao, C. Sun, W. Li, L. Yang, F. Jin, Y. Hui, H. Li, X. Wang, and K. Dong, Field-free spin–orbit torque switching in $L1_0$-FePt single layer with tilted anisotropy, *Appl. Phys. Lett.* 120(10), 102405 (2022)